

Effect of the epikarst on the hydrograph of karst springs : a numerical approach

*Laszlo Kiraly**, *Pierre Perrochet*** and *Yvan Rossier****

ABSTRACT

Most theoretical and practical problems in karst hydrogeology are related to, or depend on, the organized heterogeneity of karst aquifers. Rapidly reacting karst springs show evidence of the effect of this heterogeneity on infiltration and groundwater flow processes. The generally observed dilution effect of storm or snowmelt events on the spring-water chemistry suggests that infiltrations should be drained rapidly toward the high permeability karst network and spring. A question remains however: will the infiltrated water percolate through the low permeability fractured volumes or is it necessary to admit the existence of a "skin" of more permeable epikarst at shallow depth? This is the problem what we have been tackling with 3-D (three dimensional) groundwater flow models in the framework of the Swiss COST 65 project.

According to the first results, the proportion of the infiltrations drained by the epikarst greatly influences the general shape of the spring hydrograph, the baseflow component, the variation of the hydraulic heads (both in the karst channels and in the low permeability volumes), as well as the recharge of the low permeability volumes. The model results also suggest, that the effect of epikarst depends on many other factors and parameters as well: the hydraulic conductivity of the karst channels, the position of the channel network with respect to the spring level, extent and hydraulic parameters of the epikarst itself, etc. The comparison of the simulated spring hydrographs shows, however, clearly that the existence of epikarst is nearly always necessary to rapidly drain the infiltrations toward the karst channel network and the spring.

KEY-WORDS

Karst hydrogeology, finite element models, epikarst, spring hydrograph, baseflow, recession curve.

RÉSUMÉ

La plupart des problèmes, théoriques ou pratiques, de l'hydrogéologie du karst sont liés à l'hétérogénéité organisée des aquifères karstiques. La variation rapide du débit, ainsi que l'effet de dilution sur le chimisme des eaux généralement observés aux sources karstiques en période de recharge, laissent supposer que les infiltrations sont drainées rapidement vers le réseau karstique très perméable et la source. Le mécanisme de drainage reste, toutefois, sujet à controverse: est-ce que des infiltrations diffuses percolent à travers les volumes de calcaire fissuré peu perméable, ou faut-il admettre l'existence d'une zone d'épikarst, c'est-à-dire d'une zone "cutanée" plus perméable qui conduirait les infiltrations rapidement vers le réseau karstique à faible profondeur déjà. C'est le problème que nous avons abordé dans le cadre du projet suisse de COST 65 à l'aide de modèles d'écoulement tridimensionnels à éléments finis.

* Université de Neuchâtel, Centre d'hydrogéologie, Rue Emile-Argand 11, CH-2007 Neuchâtel

** Ecole polytechnique fédérale de Lausanne, GEOLEP, CH-1015 Lausanne

*** Dir. régionale de l'environnement, Service de l'eau et des milieux aquatiques, F-21067 Dijon

Les premiers résultats indiquent que la quantité des infiltrations drainées par l'épikarst influence non seulement la forme générale de l'hydrogramme des sources karstiques et du flot de base, mais aussi la variation des charges hydrauliques dans le réseau karstique et les volumes peu perméables, donc finalement le mécanisme de recharge de l'aquifère tout entier. L'effet de l'épikarst sur les écoulements souterrains dépend de plusieurs facteurs et paramètres: la conductivité hydraulique du réseau karstique, la position du réseau karstique par rapport au niveau des sources karstiques, de l'extension et des paramètres hydrauliques de l'épikarst, etc. La comparaison des hydrogrammes simulés montrent, toutefois, que l'existence de l'épikarst est presque toujours nécessaire pour drainer les infiltrations rapidement vers le réseau karstique et la source.

MOTS-CLÉS

Hydrogéologie du karst, modèles à éléments finis, épikarst, hydrogramme des sources karstiques, flot de base, courbe de tarissement.

1. Introduction

1.1 Definition of the problem

The organized heterogeneity of many karst aquifers may be schematized by a high permeability channel network with kilometer wide "meshes", which is "immersed" in a low permeability fractured limestone volume, and is well connected to a local discharge area, the karst spring. The **duality** of karst aquifers is a direct consequence of this structure: *duality of the infiltration processes* ("diffuse" or slow infiltration into the low permeability volumes, "concentrated" or rapid infiltration into the channel network), *duality of the groundwater flow field* (low flow velocities in the fractured volumes, high flow velocities in the channel network) and *duality of the discharge conditions* (diffuse seepage from the low permeability volumes, concentrated discharge from the channel network at the karst springs).

The behaviour of the karst spring (hydrograph, chemical or isotopic composition, etc.) represents the "*global response*" of the karst aquifer to input events. As the available data on the hydraulic parameters are very limited, the more easily obtained global response is often used to make inferences, sometimes even contradictory inferences, on the infiltration and groundwater flow processes, as well as on the hydraulic parameter fields. The rapid variation of the spring discharge and the generally observed dilution effect of storm or snowmelt events on the spring-water chemistry (figure 1) suggest, for example, that an important part of the infiltrations should be drained rapidly toward the high permeability karst channel network and the spring.

For the infiltration and drainage mechanism there are, however, at least two contradictory explanations :

- In the first it is supposed that infiltrations are mainly diffuse. The rise of the groundwater table in the low permeability fractured volumes would "press" the old water into the karst channels which rapidly conduct and discharge it at the karst spring. The high proportion of "old water component" resulting from the chemical or isotopic hydrograph separation by the method of the End Member Mixing Analysis (EMMA) seems to confirm this hypothesis and the much lower proportion of "new water component" is often identified with the "rapid recharge to the conduit system after a storm" (DREISS 1989, page 121).

- In the second explanation it is supposed that an important part of the infiltrations arrives rapidly and in concentrated form directly into the channel network. Besides the rivers disappearing in sinkholes, the concentrated infiltrations would result from the rapid drainage in a high permeability "skin" at shallow depth: the epikarst (MANGIN 1975). Earlier numerical experiments with 2-D finite element models actually showed the necessity to impose a high proportion of concentrated infiltrations in order to generate the typical "karstic" storm hydrographs (KIRALY & MOREL 1976a, 1976b), but the epikarst layer could not be explicitly included in these 2-D models.

The direct verification of the two contradictory hypotheses by field measurements is, obviously, very difficult. In order to show indirectly the consequences of the two hypotheses we explicitly introduced the epikarst layer in a 3-D finite element model and varied the proportion of the diffuse infiltrations with respect to the concentrated infiltrations resulting from the rapid drainage in the epikarst zone. As the model is transparent for the modeller, the simulated behaviour of the theoretical karst aquifer will clearly show the effect of epikarst not only on the spring hydrograph, but also on the baseflow component of the spring discharge, on the variation of hydraulic heads and fluxes during recharge and recession periods, as well as on the recharge conditions of the low permeability fractured volumes.

1.2 Brief description of the computer codes used for the simulation

The computer codes FEN1 and FEN2 have been derived from the computer code FEM301, which was previously developed at the Centre d'Hydrogéologie of Neuchâtel and submitted to severe and several verification tests under the international HYDROCOIN project (see, for example, O.E.C.D. 1988).

FEN1 and FEN2 simulate steady-state or transient, one-, two- or threedimensional saturated groundwater flow by the finite element method. The programs allow for the incorporation of one-, two- or threedimensional linear or quadratic elements within a threedimensional network and are particularly well suited for analyzing regional groundwater flow systems in highly heterogeneous geologic media (e.g. fractured or karstic aquifers).

The saturated, constant density, transient groundwater flow is represented by equation (1)

$$S_s \frac{\partial h}{\partial t} + \text{div} (-[K] \cdot \overrightarrow{\text{grad}} h) + Q = 0 \quad (1)$$

where S_s is the specific storage coefficient (1/m), $[K]$ is the hydraulic conductivity tensor (m/s), h is the hydraulic head (m) and Q represents the general source/sink terms.

The finite element formulation of the governing partial differential equations is done by the Galerkin method, yielding a set of linear equations. Assembling and solving of the system of linear equations is based on the frontal elimination technique of IRONS (1970), which is a particularly useful modification of the Gauss elimination procedure. The frontal method is very efficient for very large threedimensional problems and allows the modeller to rapidly introduce changes in the geometry of the model. The original code FEM301 and the frontal method are described in detail by KIRALY (1985). The time dependent problem is solved in FEN2 by using the robust Crank-Nicholson implicit time-stepping scheme.

UFEN1 is a code derived from FEN1 and simulates one-, two- or threedimensional saturated/unsaturated steady-state groundwater flow. In this paper it is used to simulate the free groundwater table in a theoretical "shallow" karst aquifer.

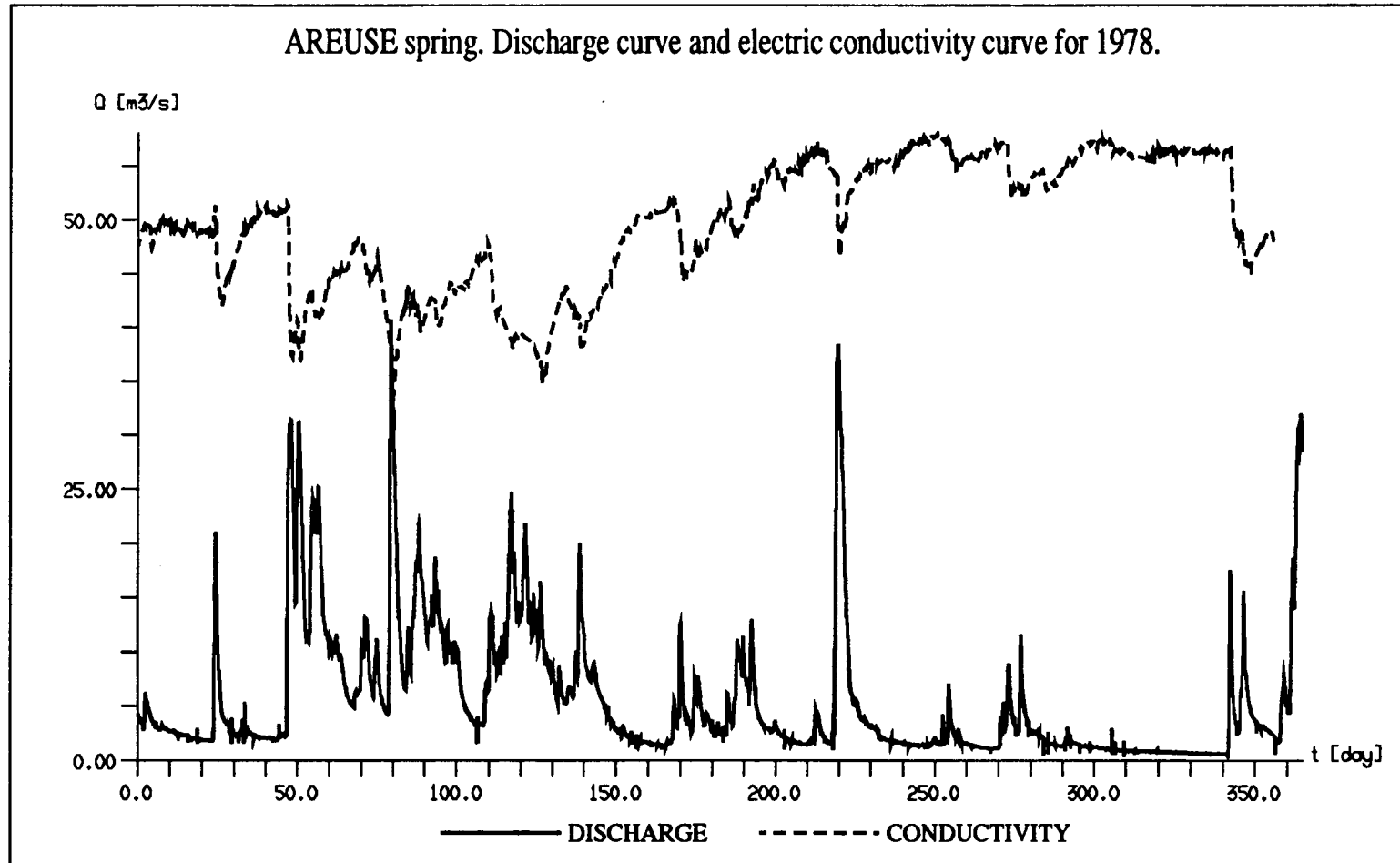


Figure 1 : Dilution effect on the spring water mineralization during recharge periodes as evidenced by the electric conductivity curve (Areuse spring, Swiss Jura Mountains). The electric conductivity values vary between 170 and 290 $\mu\text{S}/\text{cm}$.

The computer codes allow the modeller to "concatenate" several aquifers into one model. The calculated discharges of the "upstream" aquifer will be injected in the "downstream" aquifer at each time-step as variable boundary conditions. This facility is used to link the epikarst with the mean aquifer.

A slightly modified version of FEN2 offers another facility when used to simulate karst aquifers. By giving the identification number of the nodal points located on the karst channels, the program calculates the contribution of each 3-D element (i.e. low-permeability fractured volume) to the karst net. The sum of these contributions is simply the **baseflow** which can be compared to the total spring hydrograph.

2. Brief description of the theoretical karst aquifers

2.1 Karst syncline with epikarst

The diagrams of figure 2 show the 3-D geometry of a theoretical "half-syncline" drained by a very simplified high-permeability karst channel network. The karst channels are simulated by quadratic 1-D elements introduced "in sandwich" between the quadratic 3-D elements simulating the low-permeability fractured volumes.

Diagrams 2b and 2c show a steady state solution without epikarst and the drastic contrast between the rather "gentle" groundwater table and the complexity of the potential distribution in the interior of the aquifer. As a matter of fact, the knowledge of the only groundwater table would not give any information on the flow processes and on what happens in the interior of the aquifer. Note that nearly the entire volume of the mean aquifer (including the high-permeability channel network) is *below the karst spring level*, in the *saturated zone*.

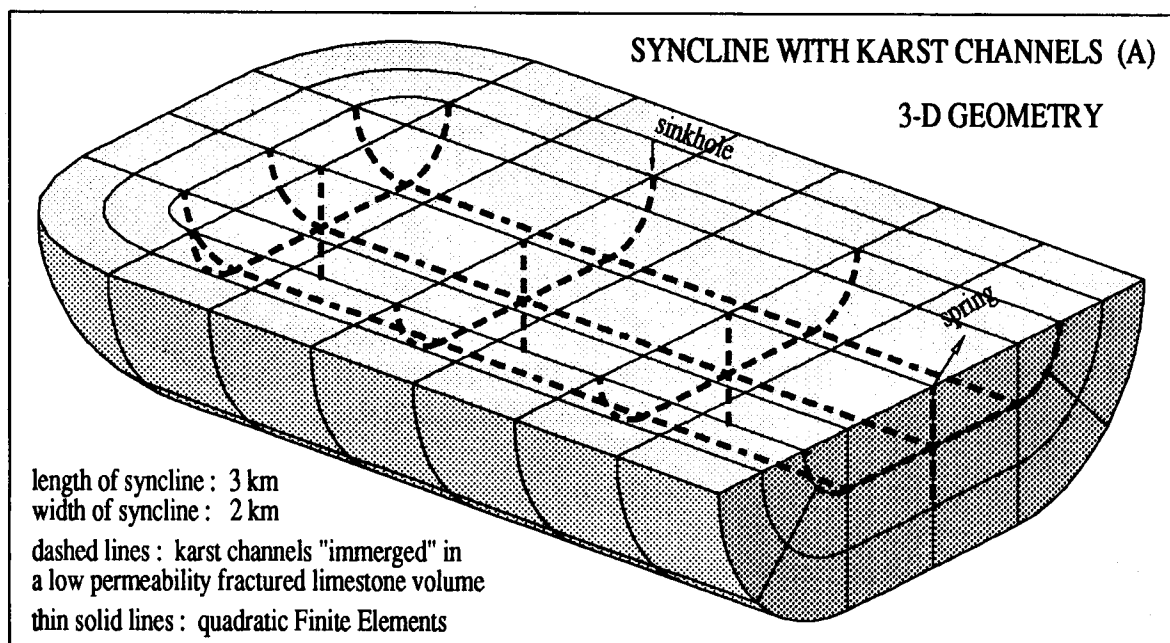
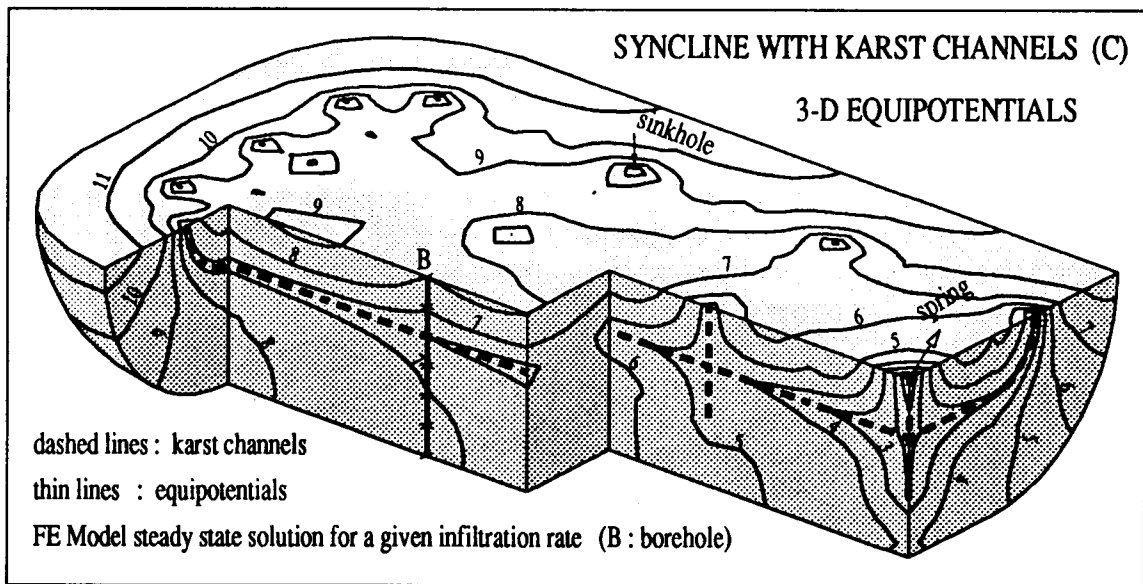
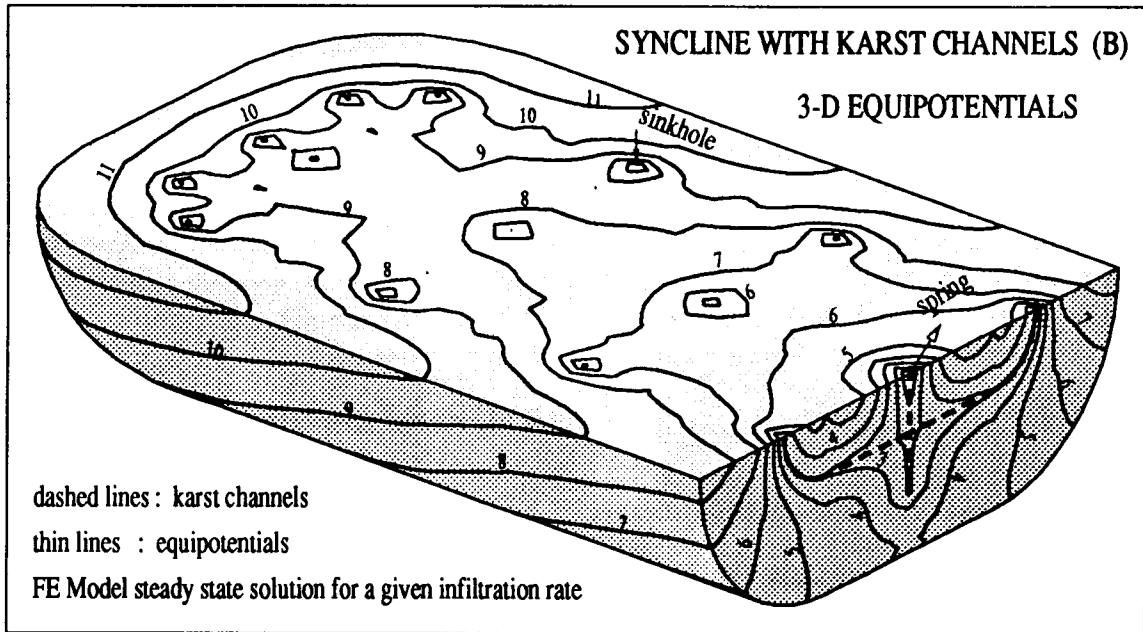


Figure 2a: Geometry and discretization of the theoretical karst syncline model.



Figures 2b and 2c: Steady state solution for a given infiltration rate obtained by the karst syncline model.

The **epikarst**, such as it was defined by MANGIN (1975), is itself a very complicated hydrogeologic unit (figure 3) and might play several roles in the infiltration and groundwater flow processes (MANGIN 1975, page 93) :

- It hinders the surface runoff by absorbing and storing the rainfall and snowmelt water.
- Depending on its horizontal permeability it may rapidly drain the stored water toward the enlarged fractures or karst channels and thus enhance the "concentrated" infiltrations.
- The remaining stored water may contribute to the "diffuse" recharge of the low-permeability fractured volumes, or may form a more or less temporary saturated zone at shallow depth.

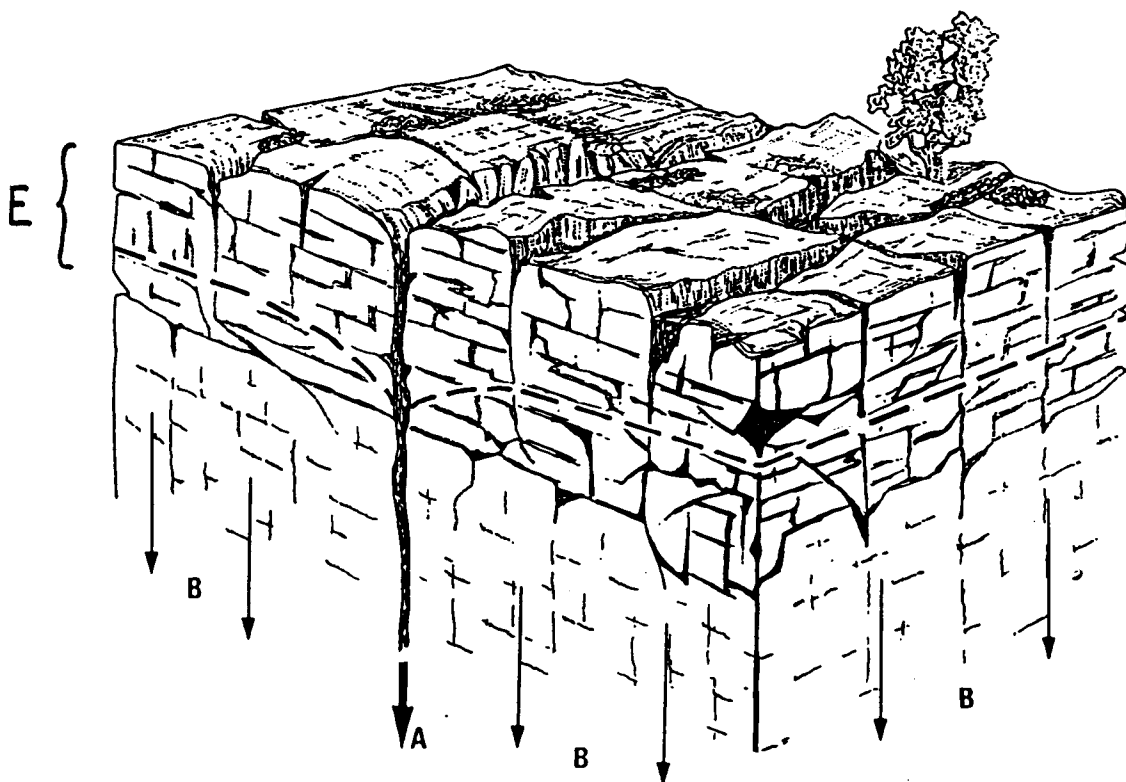


Figure 3 : Schematic representation of the epikarst zone (E) after MANGIN (1975), with concentrated (A) and diffuse (B) infiltrations.

In the present paper we are interested only in its role of enhancing the concentrated infiltrations. It is simulated by a 2-D finite element layer which will discharge into the channel network of the 3-D syncline, such as represented in figure 4. The hydraulic heads are imposed at the base of the epikarst model (where the channels intersect the 2-D layer), and the calculated discharges are injected at each time-step into the channel network of the 3-D model. This will represent the *concentrated infiltration function* for the mean aquifer.

The *diffuse infiltrations* are imposed directly onto the surface of the 3-D model because the unsaturated zone is not simulated in the case of this theoretical syncline. This represents an important simplification, but our aim was to obtain a rapid and rather "qualitative" indication on the effect of the concentrated infiltrations.

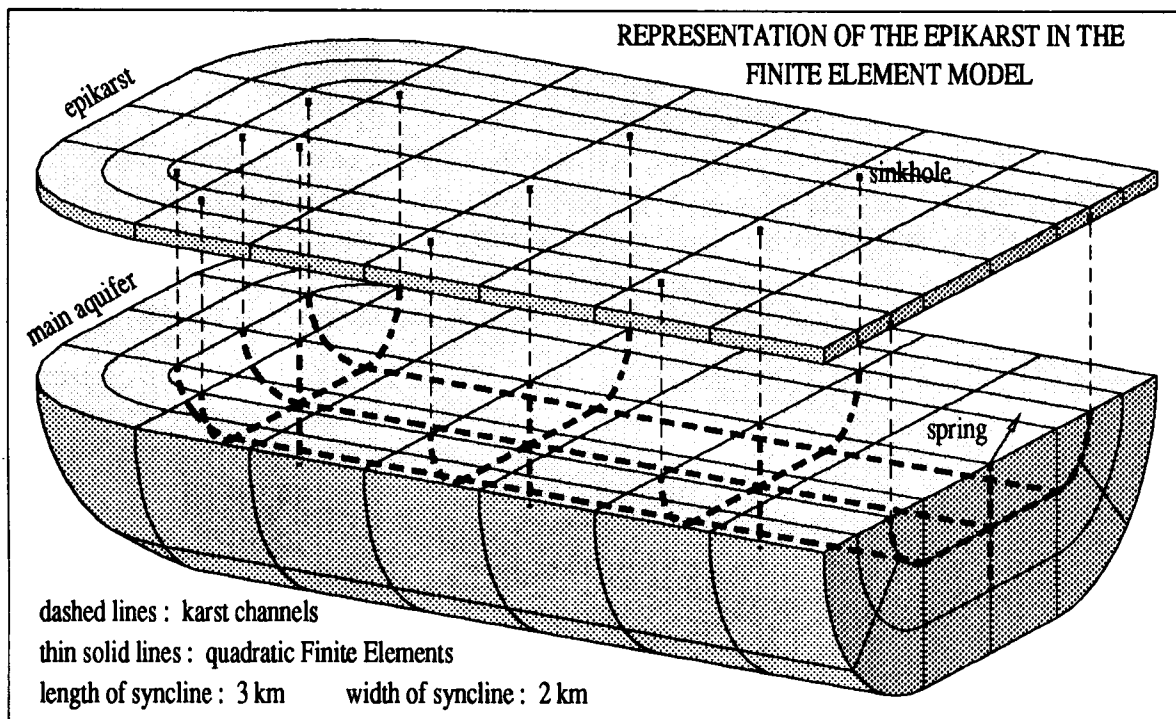


Figure 4 : Representation of the epikarst in the finite element model.

2.2 Shallow karst aquifer with unsaturated karst channels

Figure 5 represents a small "shallow" karst aquifer with an important vertical exaggeration. The aquifers of this type generally develop on plateaus or gently dipping cuestas. In the theoretical aquifer represented in figure 5, the karst network is located above the spring level and is everywhere *unsaturated*. The channels are actually *underground rivers* and represent seepage surfaces with variable boundary conditions for the low-permeability fractured volumes. The free groundwater table was obtained by simulating the steady-state, saturated/unsaturated flow in the low-permeability volumes. The detailed results of the transient simulations will be presented in another paper.

The karst syncline described above and the shallow karst of figure 5 represent two extremes and their reaction to important concentrated infiltrations will not be the same. The aim of including the "shallow karst" configuration in this paper is to remind the reader of the diversity of karst aquifers and to avoid abusive generalizations of the results obtained by the saturated karst syncline model (see subsection 3.4).

2.3 Remarks on the geometry, the discretization and the hydraulic parameters used in the model

The geometry of the karstic syncline represented in figure 2a is not realistic: the horizontal extension is too small (about 6 km²) with respect to its vertical dimension. Unfortunately it was the only way to keep the figures easily readable.

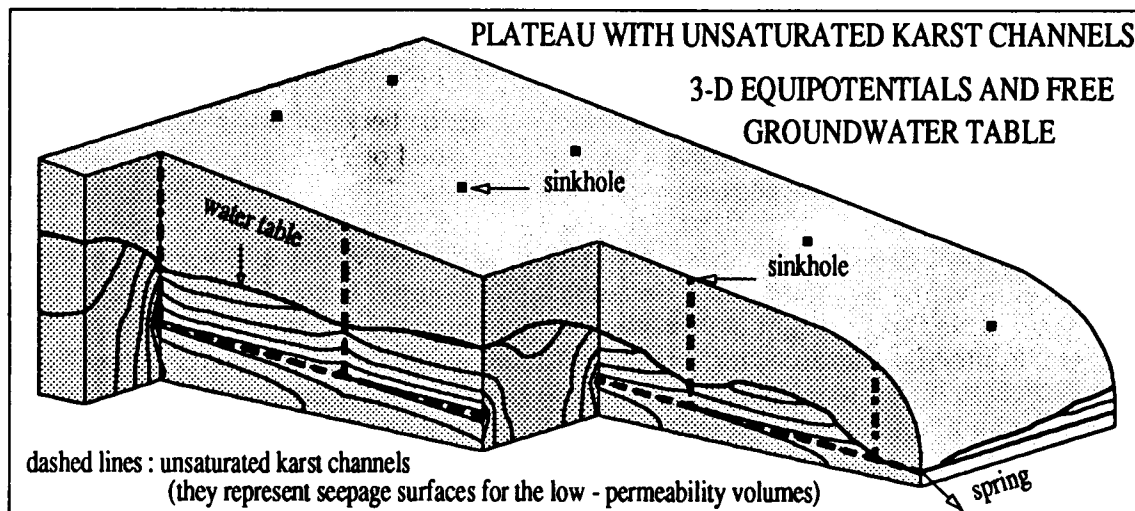


Figure 5 : Shallow karst aquifer model, with unsaturated karst channels.

The discretisation of the modelled region in finite elements is too coarse: there are only 232 lagrangian quadratic elements and 1428 nodal points in the model. The obtained results seem however quite acceptable, although a finer discretization would have been preferable.

The hydraulic parameters are the same for all variants presented in chapter 3. The hydraulic conductivities K are realistic: $5 \cdot 10^{-6}$ [m/s] for the low-permeability fractured volumes and 100 [m/s] for the high-permeability karst channels. In the 2-D epikarst layer the transmissivity T is relatively high: about $5 \cdot 10^{-2}$ [m²/s]. Linear Darcy's law is used throughout the models. The specific storage coefficients S_s are kept artificially low in order to "accelerate" the evolution of the simulated hydraulic head and flow field. In the channel network the values of S_s are 400 to 500 times higher than in the low-permeability fractured volumes.

The "shallow" karst aquifer of figure 5 is somewhat finer discretized than the above described karstic syncline: there are 750 lagrangian quadratic elements and 5859 nodal points in the model.

Finally it must be emphasized that we use in both models a very simplified karst channel network. In real systems the karst network is hierarchically organized, with lower and higher order branches having lower and higher hydraulic conductivity values. In the above described models all branches of the karst network are of the same order of magnitude and have the same hydraulic conductivity.

2.4 Remarks on the infiltration functions used in the model

Figure 6 represents the intensity of the infiltrations for three input events ("storms"), of a duration of 24 hours each. During the first and second event the infiltrations are distributed over the whole syncline. During the third "storm", infiltration takes place only on a small stripe in the middle part of the model, representing about 30% of the total infiltration area.

The volume of the total infiltrations remains the same in each variant, but the proportion of the diffuse and concentrated infiltrations will change from one variant to another. Four cases have been simulated :

DSYN0 :	100%	diffuse infiltration	0%	drained by the epikarst
DSYN20 :	80%	diffuse infiltration	20%	drained by the epikarst

DSYN50 : 50% diffuse infiltration 50% drained by the epikarst
 DSYN100 : 0% diffuse infiltration 100% drained by the epikarst

Now, we have to insist on a rather cumbersome distinction between two terms, which play a very important role in the hydrograph separation method of MANGIN (1975). We have already pointed out, that concentrated *infiltrations* into the channel network result from the rapid drainage of the *infiltrations* into the epikarst zone. We used twice the term *infiltrations* with two different meanings: as input of storm water into the epikarst (the duration of which is 24 hours in our variants), and as output from the epikarst and input into the channels (which might have a much longer duration). Figure 7 represents the two different "infiltration" functions for variant DSYN100. In the hydrograph separation method of MANGIN (1975) the term "duration of the infiltrations" corresponds to the duration of the concentrated infiltrations from the epikarst into the high-permeability channel network.

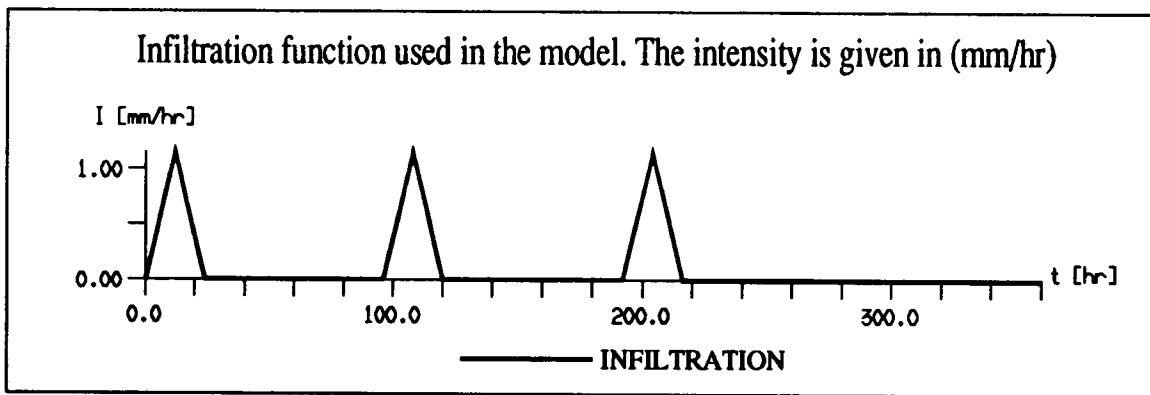


Figure 6 : Infiltration function used in the karst syncline model. The intensity I is given in mm/hr.

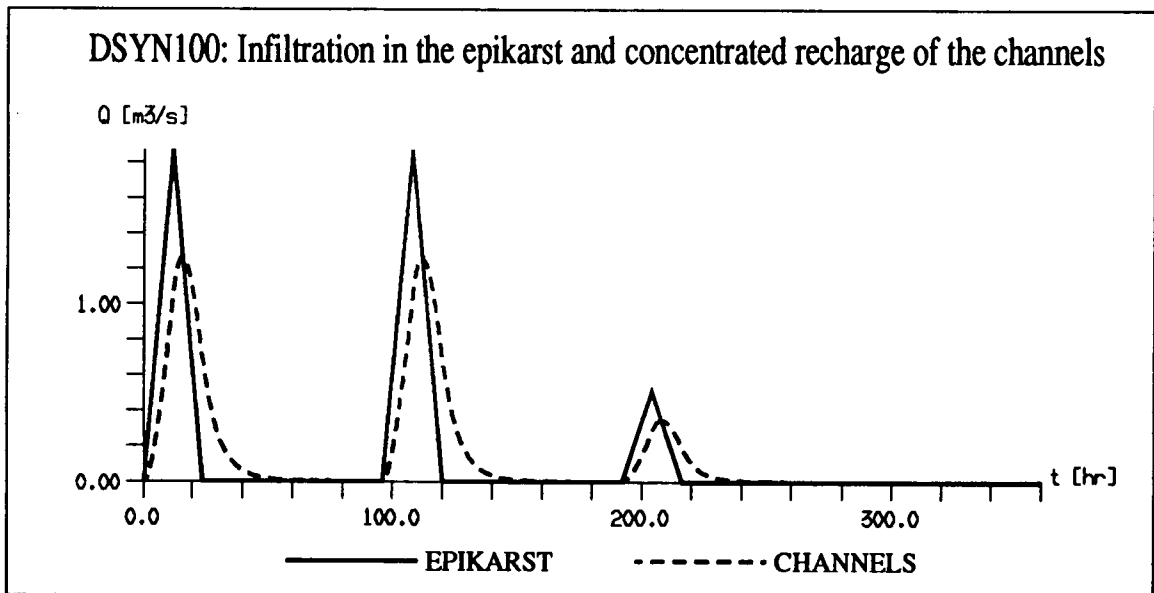


Figure 7 : Total recharge function of the epikarst and concentrated recharge function of the karst channels for variant DSYN100.

3. Presentation and discussion of the results

3.1 Effect of the epikarst on the shape of the spring hydrograph

Figure 8 is self-explanatory: it represents the spring hydrographs for different proportions of infiltration drained by the epikarst into the high-permeability channel network. It appears clearly that without some kind of concentrated infiltrations we cannot simulate the typical karstic reactions of the spring. The rise of the groundwater table in the low-permeability volumes cannot "press" enough water into the karst channels to cause a typical karstic storm hydrograph at the spring. It seems reasonable to admit that in most "open" karst aquifers more than 40% of the infiltrations should be drained rapidly into the karst channels (also see KIRALY & MOREL 1976a).

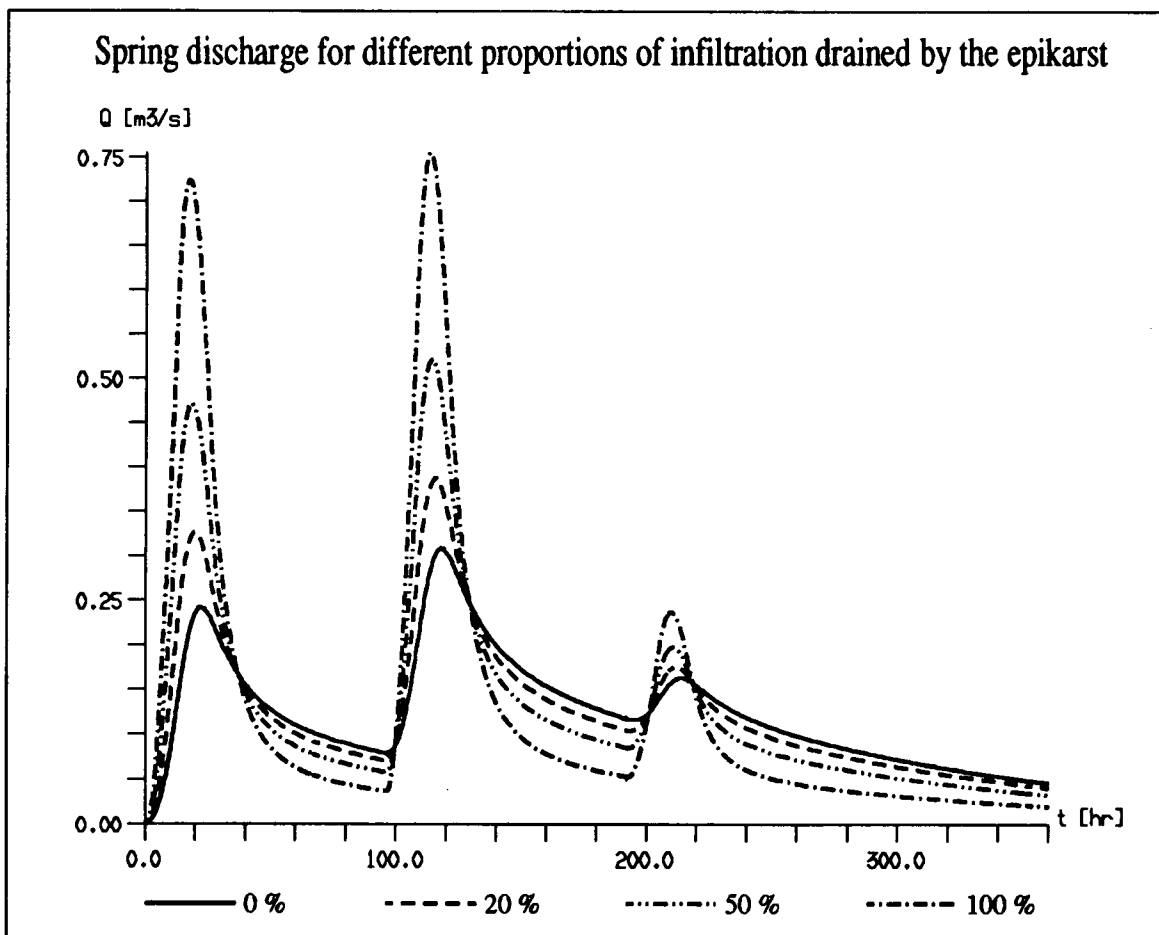


Figure 8 : Simulated spring hydrographs for different proportions of infiltration drained by the epikarst.

The high proportion of "old water" component obtained by the method EMMA (End Member Mixing Analysis) does not represent a serious argument against important concentrated infiltrations into the channel network, because the method is not related to any

consistent groundwater flow model. Indeed, in the period preceeding the storm event an important quantity of "old water" may be stored not only in the epikarst zone and in the unsaturated zone, but also in the high-permeability karst network itself, at least in the channels located below the spring level. This "old water" flows out rapidly during the peak discharge, even if the low-permeability fractured volumes do not contribute to the peak-flow at all.

Figures 18a and 18b show, by the way, that the "new water component" obtained by the End Member Mixing Analysis could not be identified with the "rapid recharge to the conduit system after a storm", as it was stated by DREISS (1989, page 121). Indeed, the "new water component" obtained by EMMA must be always smaller than the spring discharge, but figures 18a and 18b indicate clearly that the rapid recharge into the karst channels, noted as the epiflow, may be greater (or even much greater) than the spring discharge.

3.2 Effect of the epikarst on the hydraulic heads

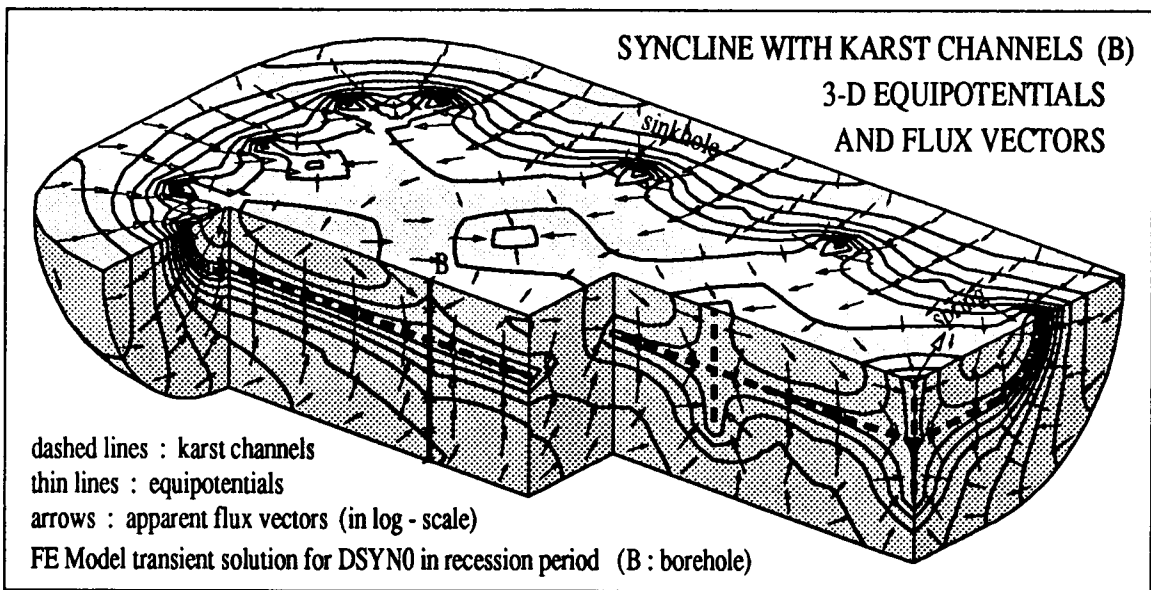
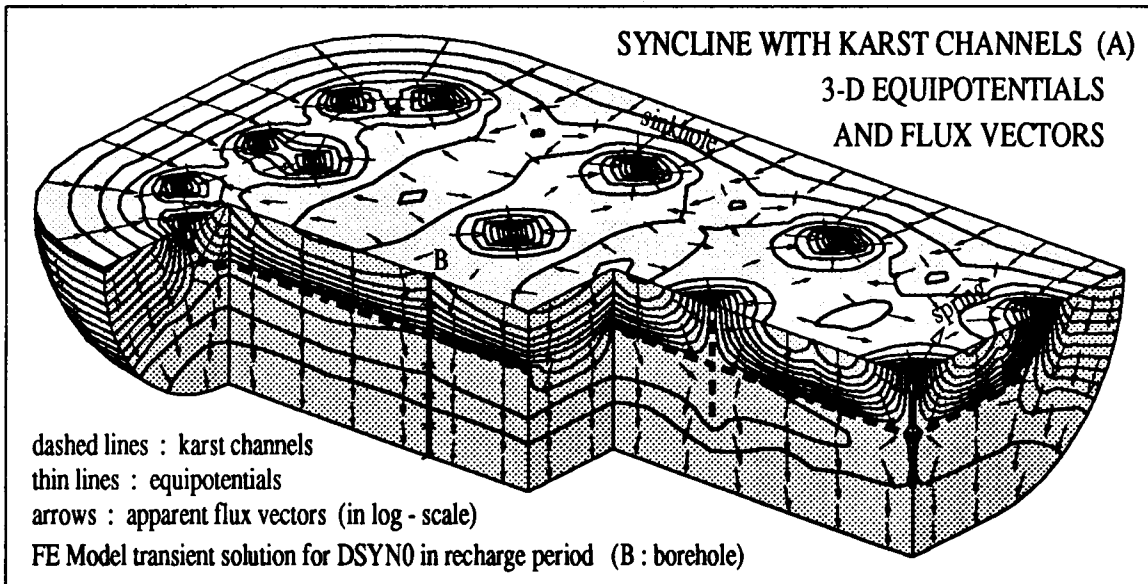
Earlier numerical experiments with 2-D finite element models suggested that concentrated infiltrations might cause an inversion of the gradients between karst channels and low-permeability volumes (KIRALY & MOREL 1976a, 1976b). These 2-D models cannot show, however, the vertical distribution of the hydraulic heads in a borehole.

Taking advantage of the 3-D model, we "registered" the simulated heads in an imaginary borehole "B", the location of which is presented in figure 2c. The borehole intersects a karst channel and the hydraulic heads are measured at 7 points between the top and the base of the aquifer.

The results are represented for the two "extreme" variants DSYN0 (no concentrated infiltrations, see figures 9a, 9b and 10) and DSYN100 (100% of the infiltrations are concentrated, see figures 11a, 11b and 12), as well as for the "reasonable" variant DSYN50 (50% of the infiltrations are concentrated and 50% are diffuse, see figure 13). Again, the figures are self-explanatory and do not need many comments.

During the recharge period there is nearly always an inversion of gradients between the karst channel and the low-permeability volumes located *below* the channel. The concentrated infiltrations must be really important to produce the same inversion with respect to the low-permeability volumes located *above* the channel. The blockdiagrams of figures 9a, 9b, 11a and 11b clearly show the recharge and drainage mechanism with and without epikarst: the most striking differences appear in the recharge periods.

The practical consequences of these theoretical results are important: the hydraulic heads should be measured separately in the high-permeability segments and in the low-permeability segments of the boreholes or piezometers. If we measure only one "groundwater level" in an otherwise heterogeneous borehole, the results will be rather misleading than helpful. Other practical consequences are related to the determination of the baseflow component, to the recharge mechanism of the low permeability fractured volumes, to the interpretation of the chemical or isotopic composition of the spring-water, etc.



Figures 9a and 9b : Transient solutions for variant DSYN0 in recharge (9a) and in recession (9b) periods.

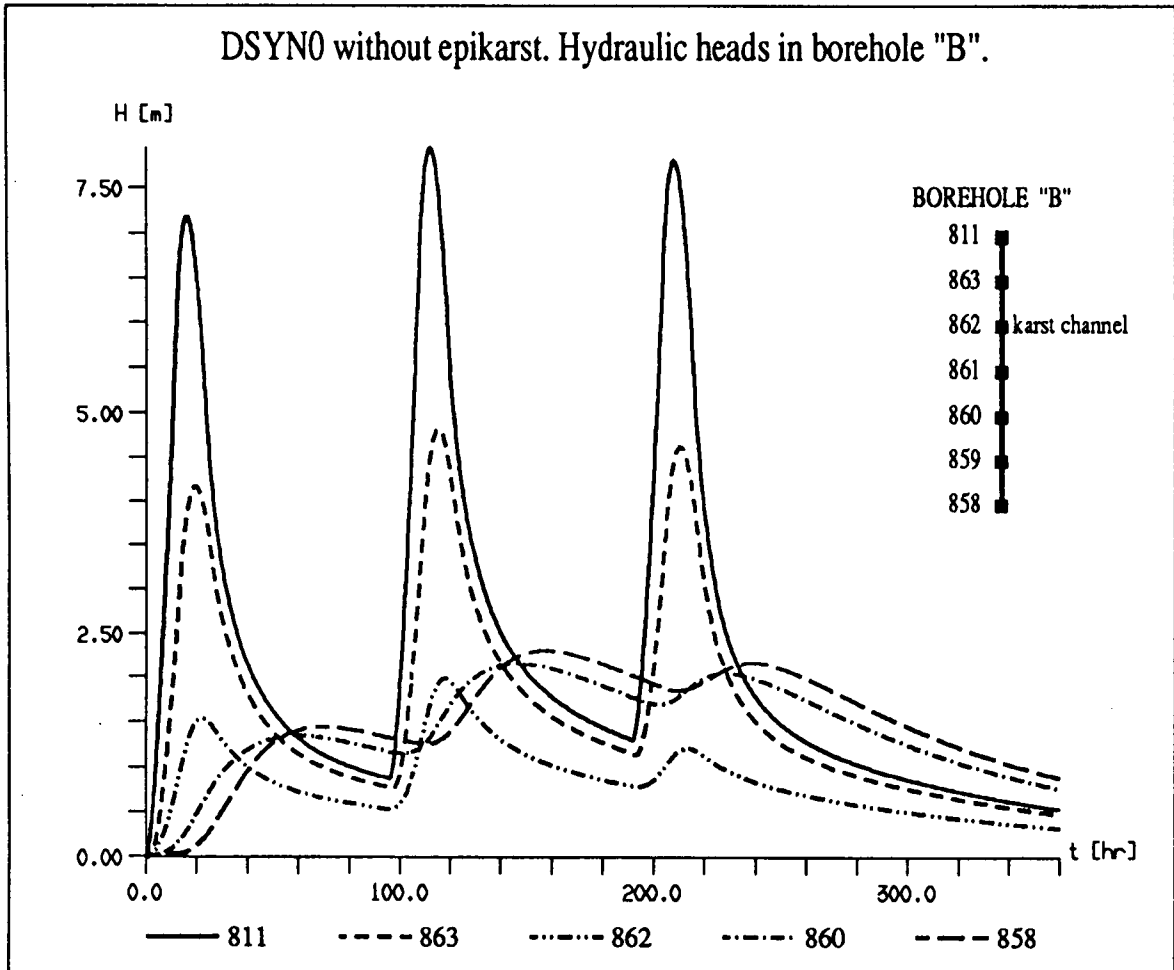
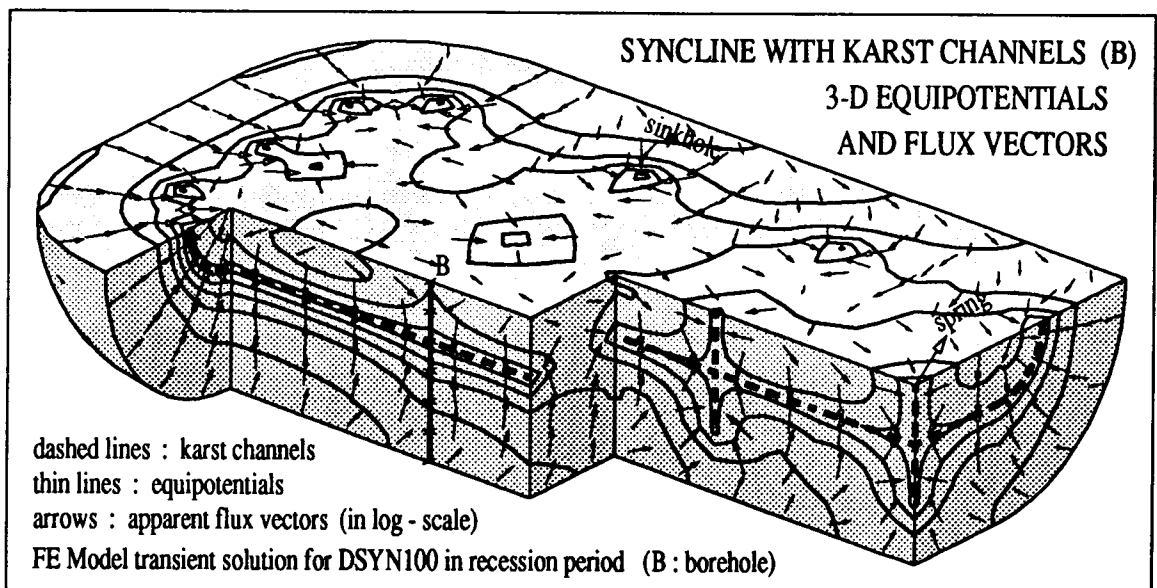
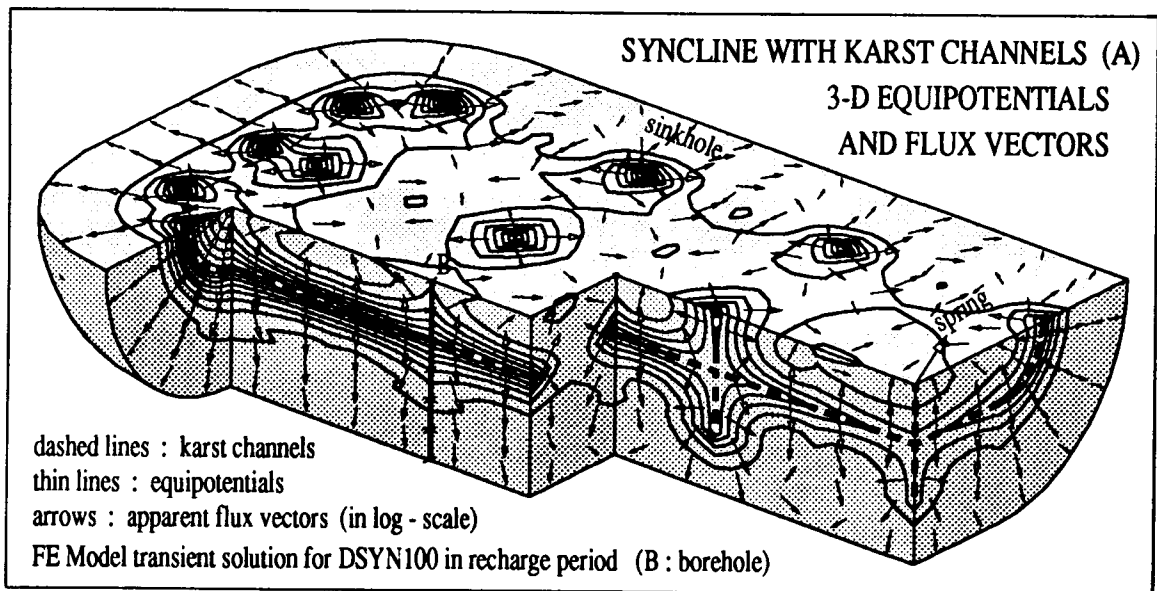


Figure 10 : Variation of the hydraulic heads in borehole "B" for variant DSYN0 (0 % drained by the epikarst).

3.3 Effect of the epikarst on the "baseflow" component of karst springs

In spite of the fact, that the inversion of gradients between karst channels and low-permeability volumes is well known by many karst hydrogeologists, most of the graphically obtained baseflow hydrographs do not show the logical consequence, namely the zero (or negative) baseflow value during recharge periods. One of the few exceptions is found in TRIPET (1973), who suppressed the baseflow component of the Areuse spring during the recharge periods.



Figures 11a and 11b : Transient solutions for variant DSYN100 in recharge (11a) and in recession (11b) periods.

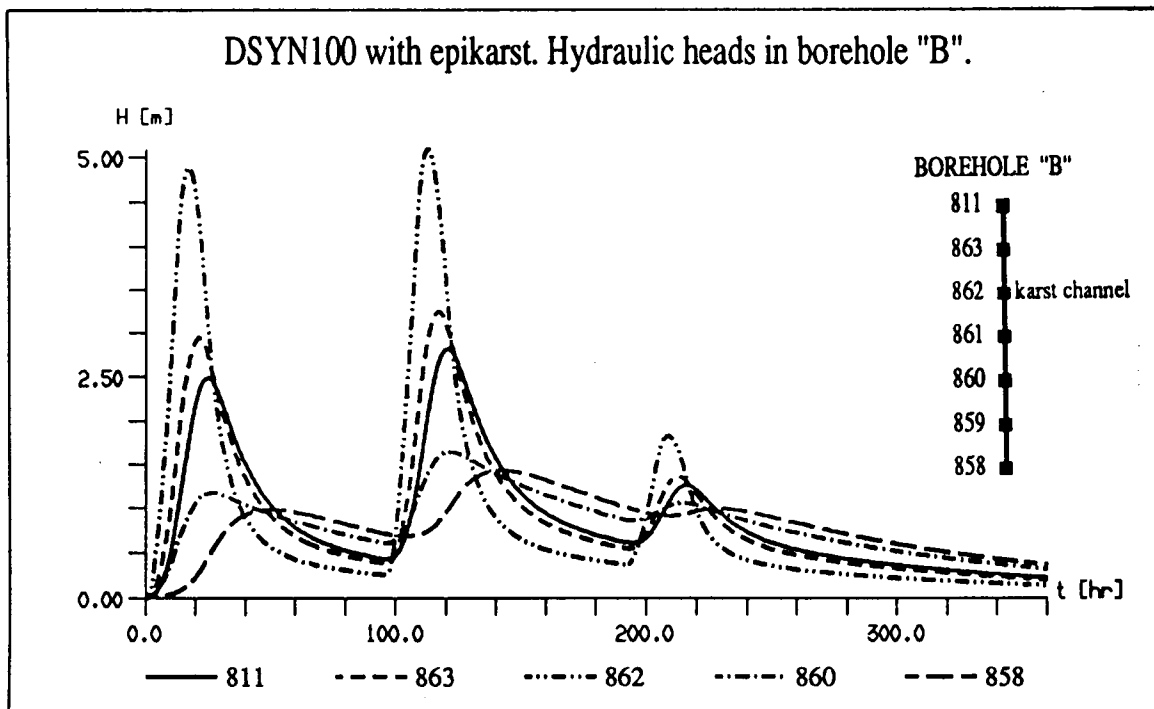


Figure 12 : Variation of the hydraulic heads in borehole "B" for variant DSYN100 (100 % drained by the epikarst).

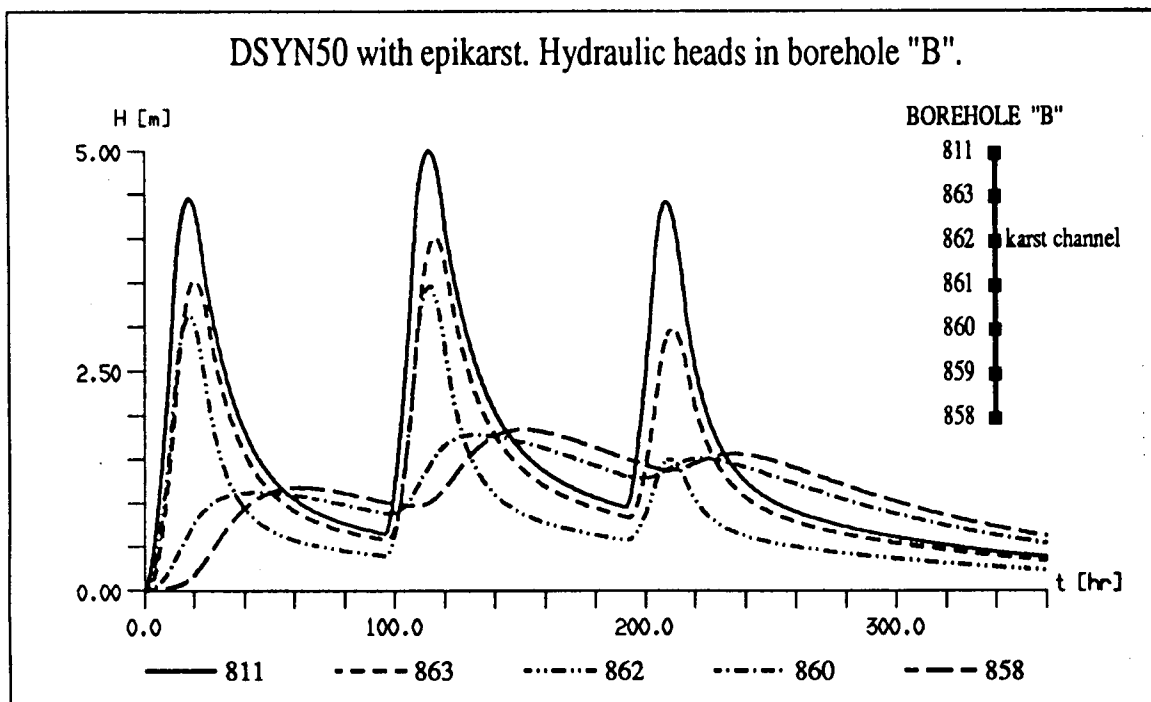


Figure 13 : Variation of the hydraulic heads in borehole "B" for variant DSYN50 (50 % drained by the epikarst).

Taking advantage of the possibility to calculate the contribution of the low-permeability 3-D elements to the nodes located on the 1-D karst channels, we computed the baseflow component for each variant. The dramatic effect of the concentrated infiltrations on the baseflow component is presented in figures 14, 15, 16 and 17 for the variants DSYN0, DSYN20, DSYN50 and DSYN100.

The appearance of negative baseflow during the recharge period indicates that the karst channels inject more water into the low-permeability volumes than they drain. The volume of this recharge might not be very important, but the fact that the low-permeability volumes may be recharged "from the interior" should not be overlooked.

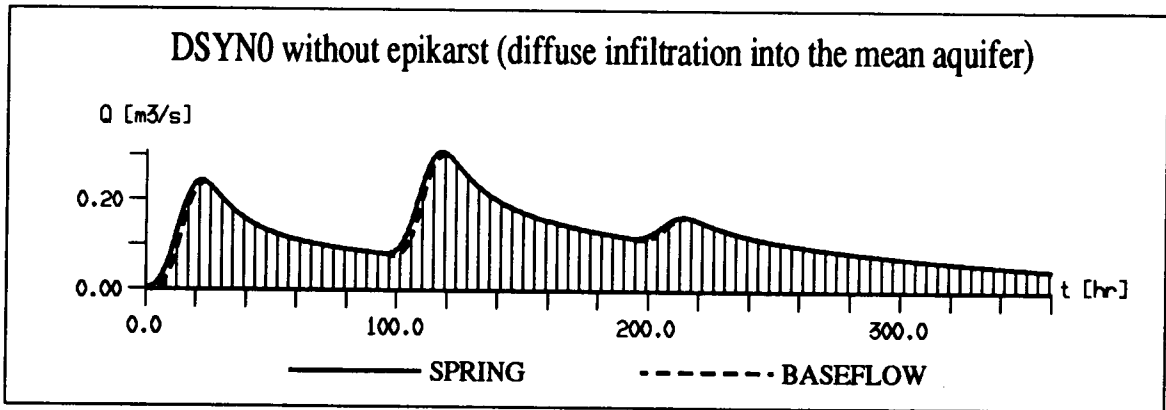


Figure 14 : Springflow and baseflow hydrographs for variant DSYN0 (diffuse infiltration into the mean aquifer).

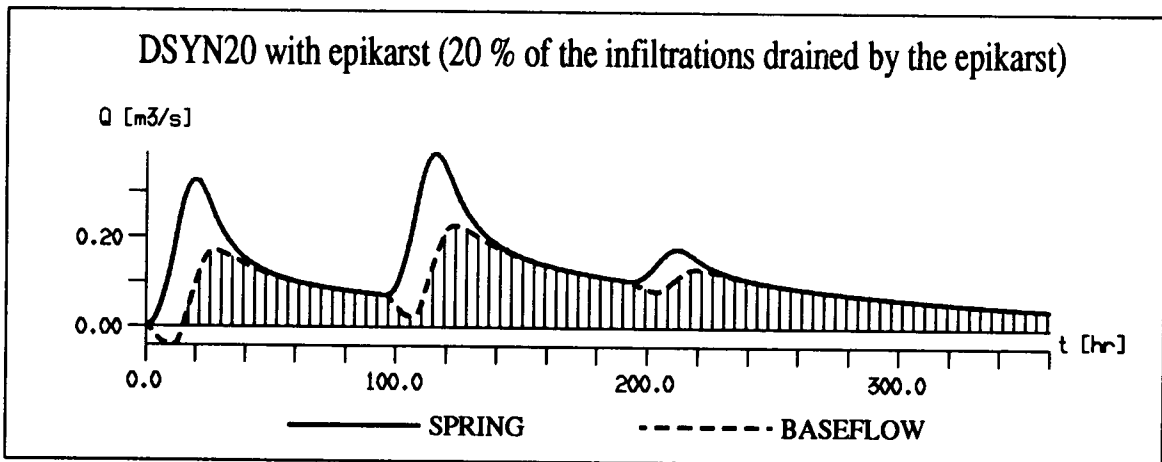


Figure 15 : Springflow and baseflow hydrographs for variant DSYN20 (20 % of the infiltrations drained by the epikarst).

Another consequence of the negative baseflow appears when estimating the "rapid infiltrations" from the spring hydrograph. Generally this is done by subtracting the graphically determined baseflow component from the total discharge curve (see for example JEANNIN & GRASSO 1995, this volume, or MANGIN 1975). Now, when the baseflow is negative, it should be added to the spring discharge, otherwise the intensity of the rapid or direct infiltrations will be systematically underestimated (see for example, figures 18a and 18b).

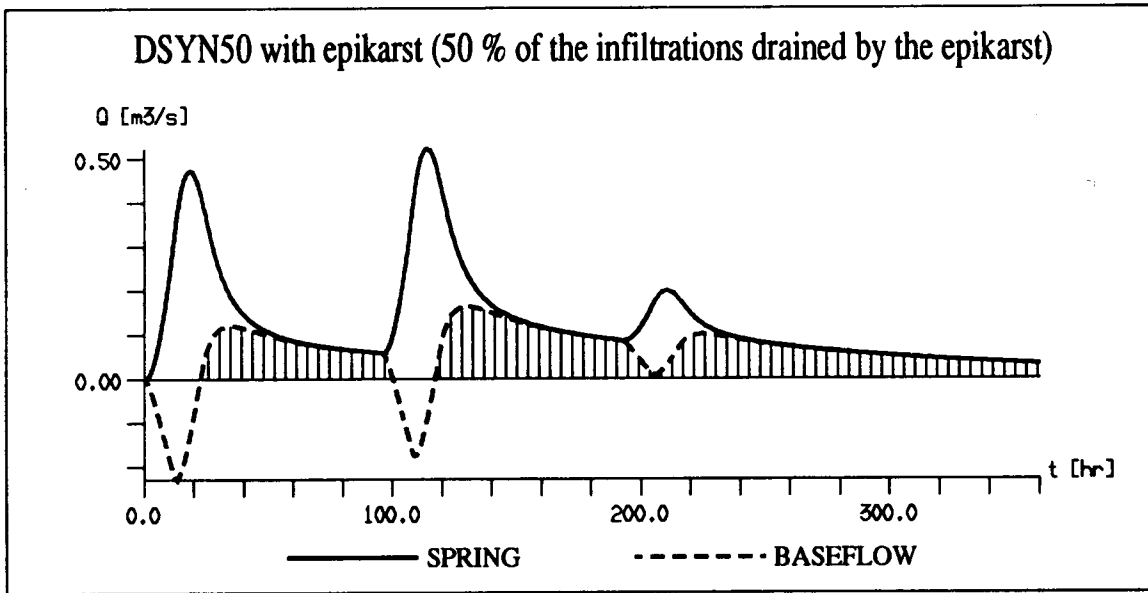


Figure 16 : Springflow and baseflow hydrographs for variant DSYN50 (50 % of the infiltrations drained by the epikarst).

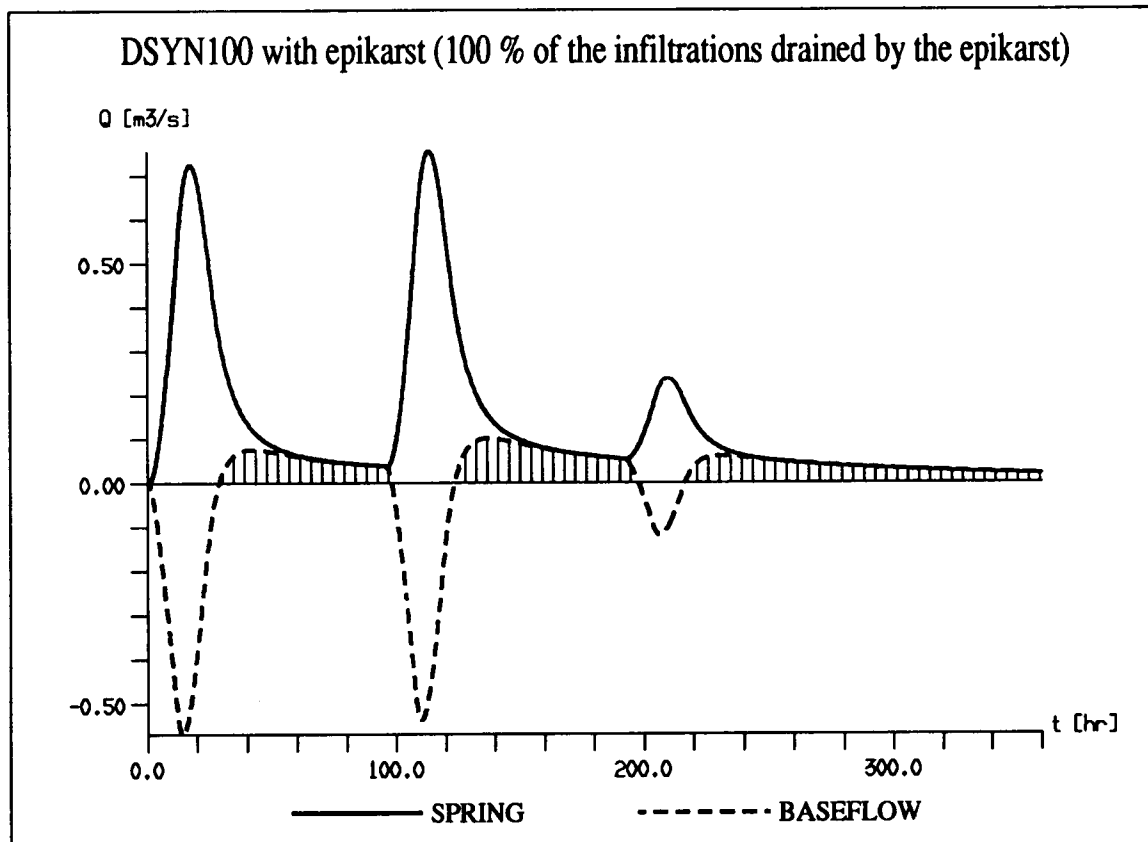


Figure 17 : Springflow and baseflow hydrographs for variant DSYN100 (100 % of the infiltrations drained by the epikarst).

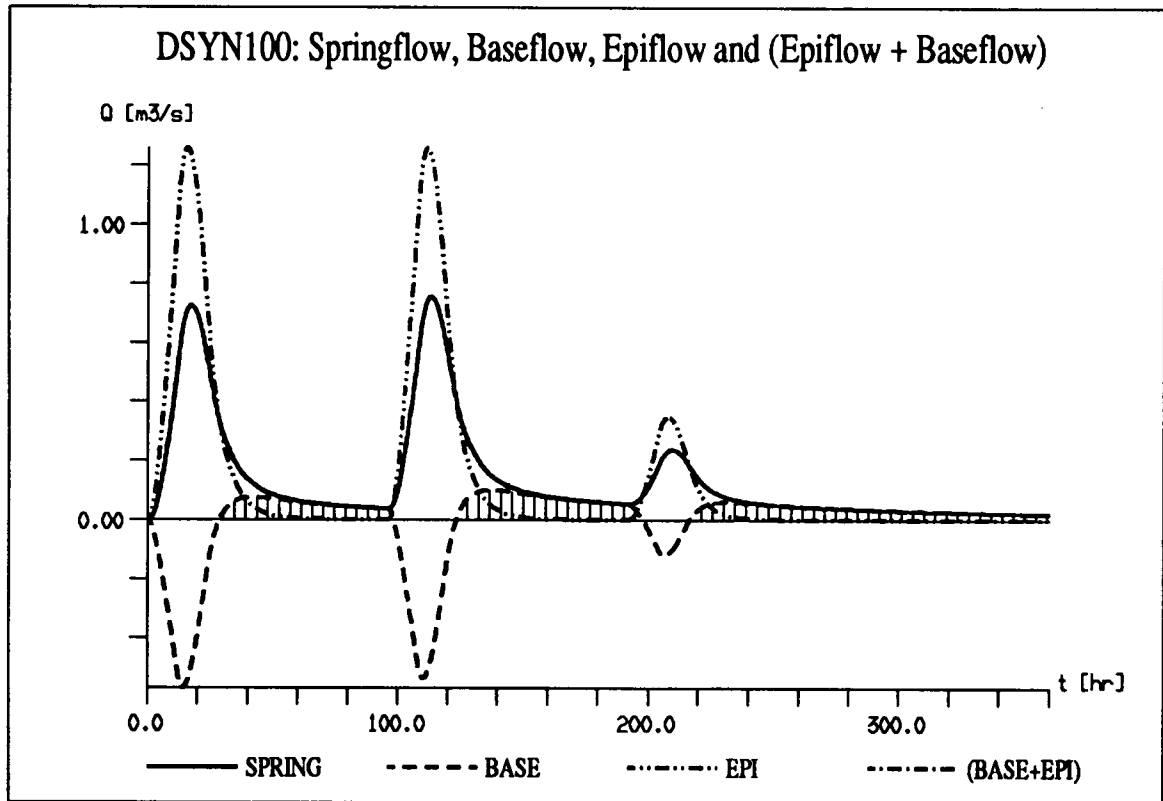


Figure 18a : Springflow, baseflow, epiflow and the sum of epiflow + baseflow for variant DSYN100.

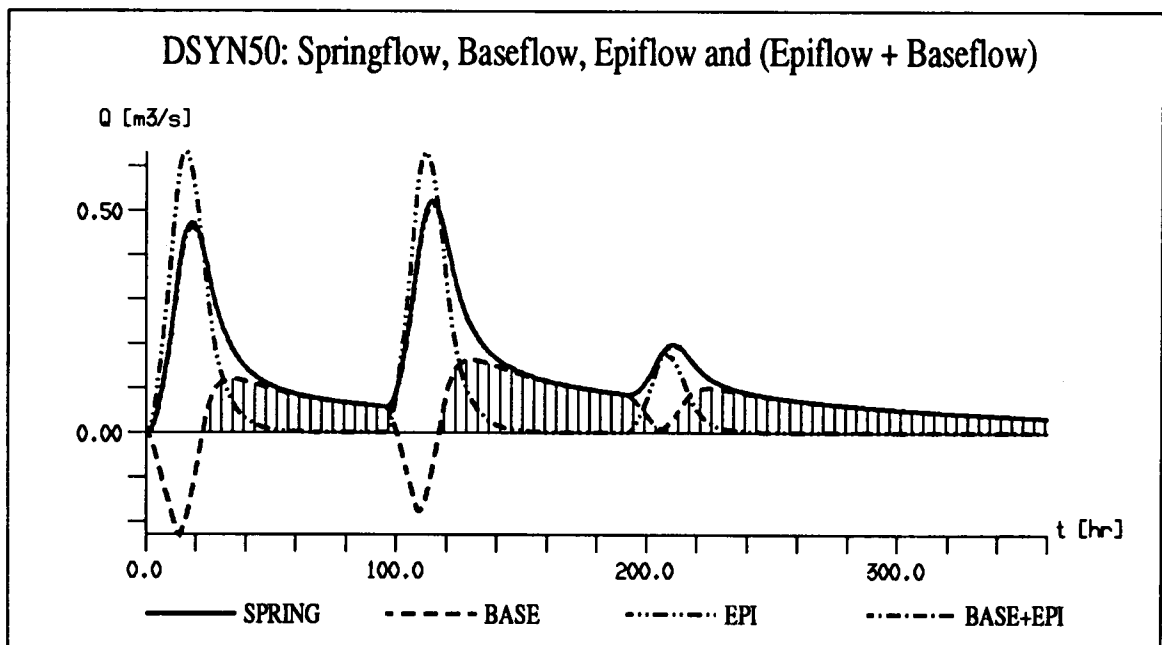


Figure 18b : Springflow, baseflow, epiflow and the sum of epiflow + baseflow for variant DSYN50.

As the model allows for the independent estimation of the baseflow and of the rapid or concentrated infiltrations into the karst channel network (which will be called "epiflow", for short, in the following), we can take a critical look at the usually accepted hydrograph separation methods. Figures 18a and 18b show that the sum of the baseflow and the epiflow coincides almost exactly with the springflow hydrograph. This means that the most natural hydrograph separation method would be to separate the total spring hydrograph into an epiflow component and a baseflow component, as it was proposed (even if using different terms) by MANGIN (1975).

Usually the baseflow is identified with the last, nearly exponential part of the recession curve. In figure 19 we represented the springflow, the baseflow and the epiflow for variant DSYN50 in log-scale, where the exponential functions should appear as straight lines. In this specific case (homogeneous transmissivity field in the 2-D epikarst layer) the recession curves of the epiflow are nearly perfect exponentials for the three input events. On the other hand, the first part of the baseflow recession curves happens to be a definitely non-exponential function! Only the very last part of the baseflow hydrograph (between 300 and 360 hours) may be represented by an exponential function, when the flow field is already in a "quasi-steady" state. Subtracting this exponential function from the total spring discharge would change the form of the epiflow hydrograph and would considerably increase the apparent duration of the concentrated infiltrations.

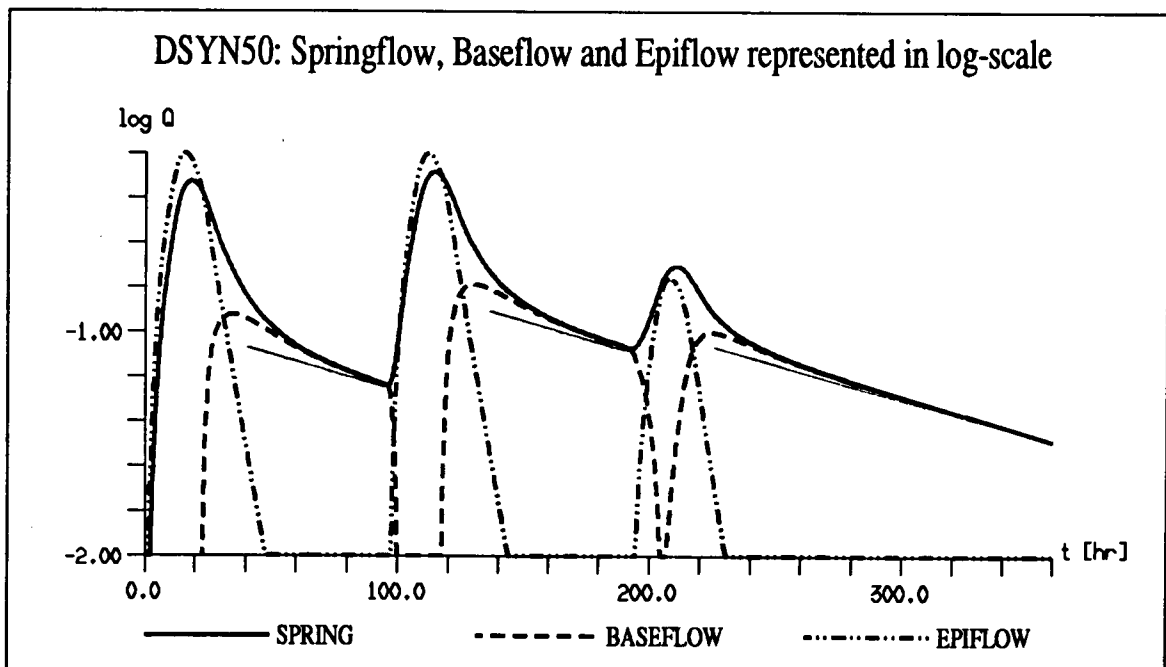


Figure 19 : Springflow, baseflow and epiflow represented in log-scale for variant DSYN50.

3.4 Remarks on the "shallow karst" configuration

In the shallow karst configuration of figure 5 the main karst channel network is located above the spring level and its hydraulic conductivity is high enough to keep the channels everywhere unsaturated, even for very important concentrated infiltrations. The most important karst channels are actually *underground rivers* and represent seepage surfaces for the low-permeability fractured volumes. Under these circumstances the concentrated infiltrations will not produce an inversion of gradients between the high-permeability karst network and the low-permeability fractured volumes, and the effect of epikarst on the hydraulic heads or on the baseflow component of karst springs will not be the same as the effects described in sections 3.2 and 3.3. Consequently, the analysis and interpretation of the spring hydrographs should also be different.

The results obtained with the shallow karst configuration will be presented in another paper. It appears, however, clearly that a reasonable interpretation of the global responses observed at the karst springs requires the knowledge of the geological and geomorphological framework of the aquifer, which represent just another (qualitative) expression for boundary conditions and hydraulic parameter fields.

3.5 Remarks on the recharge of the low-permeability volumes: the "Faraday cage" effect of the epikarst

The huge low-permeability fractured limestone volumes are often designated as the "capacitive" part of karst aquifers. They might contain important groundwater resources, and their recharge mechanism could have important practical consequences on the groundwater management problems (baseflow of karst springs, exploitation of groundwater by pumping wells or galleries, etc.).

Figure 4 ("deep" karst syncline) and figure 5 ("shallow karst") suggest that a well developed epikarst layer enhancing the concentrated infiltrations into the high-permeability karst channel network will "short-circuit" the low-permeability volumes and will play the role of a "Faraday cage" with respect to the main aquifer. Depending on the importance of this "Faraday cage" effect, the recharge of the low-permeability volumes could be much smaller than in the case of pure diffuse infiltrations, with the above mentioned important consequences on the groundwater management problems. In the "deep syncline" configuration the inversion of gradients will always contribute to recharging the low-permeability volumes "from the interior", but in the "shallow karst" configuration the "short-circuit" of the low permeability volumes might be almost complet.

4. Conclusions

Numerical experiments with a 3-D finite element model simulating the infiltration and groundwater flow processes in a highly simplified theoretical karst aquifer allowed to show the importance of the existence or non-existence of an epikarst zone. The effect of the epikarst on the hydraulic potential and the groundwater flow field has practical consequences

on the monitoring strategies applied for karst aquifers, on the interpretation of the global responses obtained at the karst springs and on the estimation of the recharge of the low-permeability "capacitive" volumes. Hydraulic head measurements should always be related to zones of known permeability and the "piezometric maps" of karst aquifers should always indicate the permeability at the measurement points.

Acknowledgements

Some of the computer codes used for the groundwater flow simulation and some of the ideas presented in this paper were developed in the framework of earlier research projects supported by the Swiss National Foundation for Scientific Research. Our most sincere thanks to this Institution.

P.-Y. Jeannin and A. Grasso (Centre d'hydrogéologie de Neuchâtel) have been spending much time on the verification of different types of model results in real aquifers. We thank them for the discussions and for the work carried out in the field. M. Razack (University of Poitiers) is acknowledged for his review and his pertinent remarks.

Last, but not least, the first author (L. Kiraly) would like to thank Alain Mangin (Moulis, France) for all the discussions (and arguments!) they have had since 25 years. Even if some of these discussions were not all that peaceful, they helped him a lot to understand more about the complexity of karst aquifers.

References

- DREISS S.J. 1989. Regional scale transport in a karst aquifer : 1. Component separation of spring flow hydrographs. *Water Resources Research*, 25, 1 : 117-125.
- IRONS B.M. 1970. A frontal solution program for finite element analysis. *Int. Journ. Num. Meth. Eng.*, 2 : 5-32.
- JEANNIN P.-Y. & GRASSO A. 1995. Recharge respective des volumes de roche peu perméable et des conduits karstiques, rôle de l'épikarst. *Bull. d'Hydrogéologie*, 14, ce volume.
- KIRALY L. & MOREL G. 1976a. Etude de régularisation de l'Areuse par modèle mathématique. *Bull. du Centre d'hydrogéologie de Neuchâtel*, 1 : 19-36.
- KIRALY L. & MOREL G. 1976b. Remarques sur l'hydrogramme des sources karstiques simulé par modèles mathématiques. *Bull. du Centre d'hydrogéologie de Neuchâtel*, 1 : 37-60.
- KIRALY L. 1985. FEM301 - A three dimensional model for groundwater flow simulation. NAGRA Technical Report 84-49, 96 pp.
- MANGIN A. 1975. Contribution à l'étude hydrodynamique des aquifères karstiques. Thèse, Univ. Dijon, 124 pp.
- O.E.C.D. 1988. The International HYDROCOIN Project. Level 1 : code verification. OECD Publications, Paris, 198 pp.
- TRIPET J.-P. 1973. Etude hydrogéologique du bassin de la source de l'Areuse. *Matér. géol. Suisse, sér. Hydrologie*, 21, 183 pp.